
MINEX III Report Card
Template Generator vsoft+0010



Last Updated: October 28, 2022

Participant Details

Company: Vsoft Tecnologia Participacoes Ltda.

Provided CBEFF PID: 007F 0010

Provided Marketing Name: "BioPassID_Extractor"

Date Application Received: 10/27/2022

Date First Submitted: 10/21/2022 (as generator version 0008)

Date Validated: 10/28/2022

Date Completed: 10/28/2022

Library	Size (bytes)	MD5 Checksum
libminexiii_vsoft_0010.so	28914040	95ab010adeaa86d97917b5221445fc18

Compliance Test Results

The following presents **PIV compliance** results per the criteria detailed in [NIST Special Publication 800-76-2: Biometric Specifications for Personal Identity Verification](#).

It also includes **MINEX III compliance** results per the criteria detailed in sections 4 through 8 of the [Minutia Interoperability Exchange \(MINEX\) III Test Plan and Application Programming Interface](#).

PIV: FAIL

- Average template creation time must be no more than 500 milliseconds (4.5.2.2-2). ✓
- Minutia density plots derived from generated templates do not exhibit a periodic, grid-like, or geometric structure. ✓
- All certified matchers must be able to match templates from this template generator with an $FNMR_{FMR}(0.01) \leq 0.01$ using two fingers (4.5.2.2-3). ✗

MINEX III: FAIL

- Must pass MINEX III validation. ✓
- Must be PIV compliant. ✗
- No more than two compliant template generators from the submitting organization, or its subsidiaries, acquisitions, or mergers allowed (8.8). ✓

Notes

- This report will be updated as new matching algorithms and template generators pass the compliance test. These updates will not change the PASS/FAIL decision above.
- NIST reserves the right to decertify a template generator if it later discovers the template generator violates MINEX III or PIV specifications in some previously undetected way.
- This submission is not compliant, and is therefore *not* a member of the pooled DET curves published throughout all MINEX III report cards.

Contents

Participant Details	1
Compliance Test Results	1
Notes	1
1 Introduction	3
2 Methodology	3
2.1 Dataset	3
2.2 Accuracy Metrics	3
2.3 Uncertainty Estimation	3
2.4 Interoperability	4
3 Results	5
3.1 Template Creation Times	5
3.2 Minutia Counts	6
3.3 Minutia Density Plots	8
4 References	9

List of Figures

1 MINEX III Interoperability Test Setup	4
2 Template Creation Times	5
3 Minutia Count Probability	6
4 Minutia Count Cumulative Summation	7
5 2D Minutia Placement Density Functions	8

List of Tables

1 Introduction

Testing is performed at a NIST facility. Each participant’s submission is validated by NIST before undergoing full testing to ensure it operates correctly. If the matcher passes the validation procedure, it is then used to compare standard fingerprint templates. Performance is assessed against templates created by a template generator submitted by the participant as well as templates created by other MINEX III compliant template generators.

2 Methodology

Testing is performed at a NIST facility. Each participant’s submission is validated by NIST before undergoing full testing to ensure it operates correctly. If the template generator passes the validation procedure, performance is assessed by using MINEX III compliant matching algorithms to compare templates created by the template generator. These matchers were submitted to the ongoing MINEX III program by various participants.

2.1 Dataset

Testing is performed over a single dataset of sequestered fingerprint images. The images were collected by U.S. Visit at ports of entry into the United States. They consist of Live-scan plain impressions of left and right index fingers. WSQ [1] compression was applied to all images at a ratio of 15:1. The most recent capture of each subject was treated as the authentication sample, and the next most recent as the enrolled sample.

The dataset was divided into 533 767 mated and 1 067 530 non-mated subject pairings. Since both left and right index fingerprints are available for each subject, this provides 1 061 657 mated and 2 127 712 non-mated single-finger comparisons (after database consolidation). When left and right index fingers are fused at the score level [3, 8], the sets condense to 530 394 mated and 1 062 814 non-mated comparison scores.

2.2 Accuracy Metrics

Core matching accuracy is presented in the form of Detection Error Tradeoff (DET) plots [7], which show the trade-off between the False Match Rate (FMR) and the False Non-Match Rate (FNMR) as a decision threshold is adjusted. Formally, let m_i ($i = 1 \dots M$) be the i th mated comparison score, and n_j ($j = 1 \dots N$) the j th non-mated comparison score. Then the statistics are

$$\text{FMR}(\tau) = \frac{1}{N} \sum_{j=1}^N \mathbb{1}\{n_j \geq \tau\}, \quad (1)$$

$$\text{FNMR}(\tau) = \frac{1}{M} \sum_{i=1}^M \mathbb{1}\{m_i < \tau\}. \quad (2)$$

where $\mathbb{1}\{A\}$ is the indicator [4] of event A . Equations 1 and 2 define the curve parametrically with the decision threshold, τ , as the free parameter. In some figures and tables, FNMR is presented as a function of FMR. This relationship is determined by

$$\text{FNMR}_{\text{FMR}}(\alpha) = \min_{\tau} \{ \text{FNMR}(\tau) \mid \text{FMR}(\tau) \leq \alpha \}, \quad (3)$$

which reads as the smallest FNMR that can be achieved while maintaining an FMR less than or equal to α , the targeted FMR. This method of relating the two error statistics ensures FNMR is well-defined for all $0 \leq \alpha \leq 1$. It also imposes a natural penalty on matching algorithms that produce heavily discretized scores.

2.3 Uncertainty Estimation

Some figures in this report include boxplots that convey the uncertainty associated with a statistic. The boxplots are intended to show the expected variation in the observed value if one assumes repeated iid sampling from the same population. They are not intended to reflect how the statistic might change over different test data or even different sampling strategies over the same data.

Estimates of uncertainty are computed using the Wilson Score method [10] which overcomes certain problems associated with applying the Central Limit Theorem to a discretized estimator. We make several simplifying assumptions when applying the method to biometric identification. Most notably, separate searches against the same enrollment database are treated as independent samples, yet we know positive correlations exist due to Doddingtons Zoo [2]. We also report estimates of the variability of FNIR at a fixed FPIR when in fact it is the decision threshold that is fixed. Uncertainty with respect to what decision threshold corresponds to the targeted FPIR results in increased uncertainty about the true value of FNIR. However, our estimates of FPIR are fairly

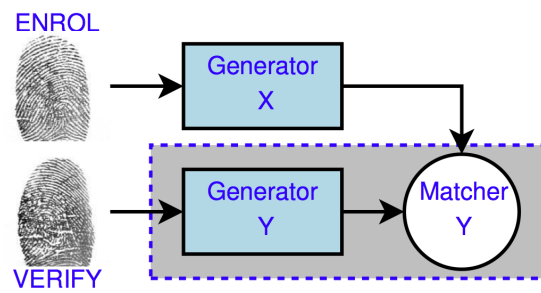


Figure 1: MINEX III Interoperability Test Setup

tight due to the large number of non-mated searches performed, so they are not expected to have a large impact on the estimates.

2.4 Interoperability

Interoperability is tested in a manner similar to *Scenario 1* from the [MINEX Evaluation Report \[5\]](#) (see Figure 1). An enrolment template is prepared using submission X. Submission Y is used to prepare the authentication template and perform the match. The authentication template is always prepared by the same submission used to compare the templates. However, enrolment templates need not originate from the same submission. When they do, we refer to as “native” mode.

3 Results

3.1 Template Creation Times

To achieve PIV compliance, the template generator must create templates in no more than 0.5 seconds (500 milliseconds) on average.

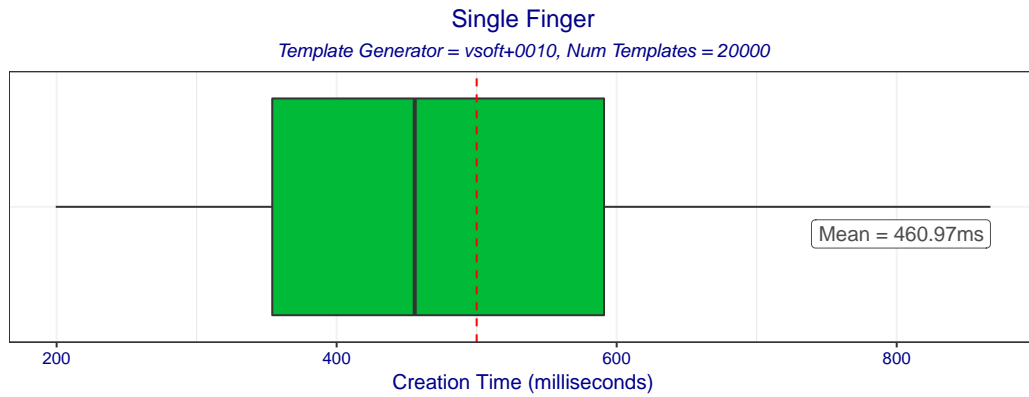


Figure 2: Boxplot of template creation times for template generator vsoft+0010. The box edges mark the 10th and 90th percentiles while the whiskers mark the maximum and minimum creation times.

3.2 Minutia Counts

This section presents information relating to the number of minutia the template generator finds in fingerprint images. The relative number of minutia found in common fingerprint images has been shown to influence matching outcomes [9, 6].

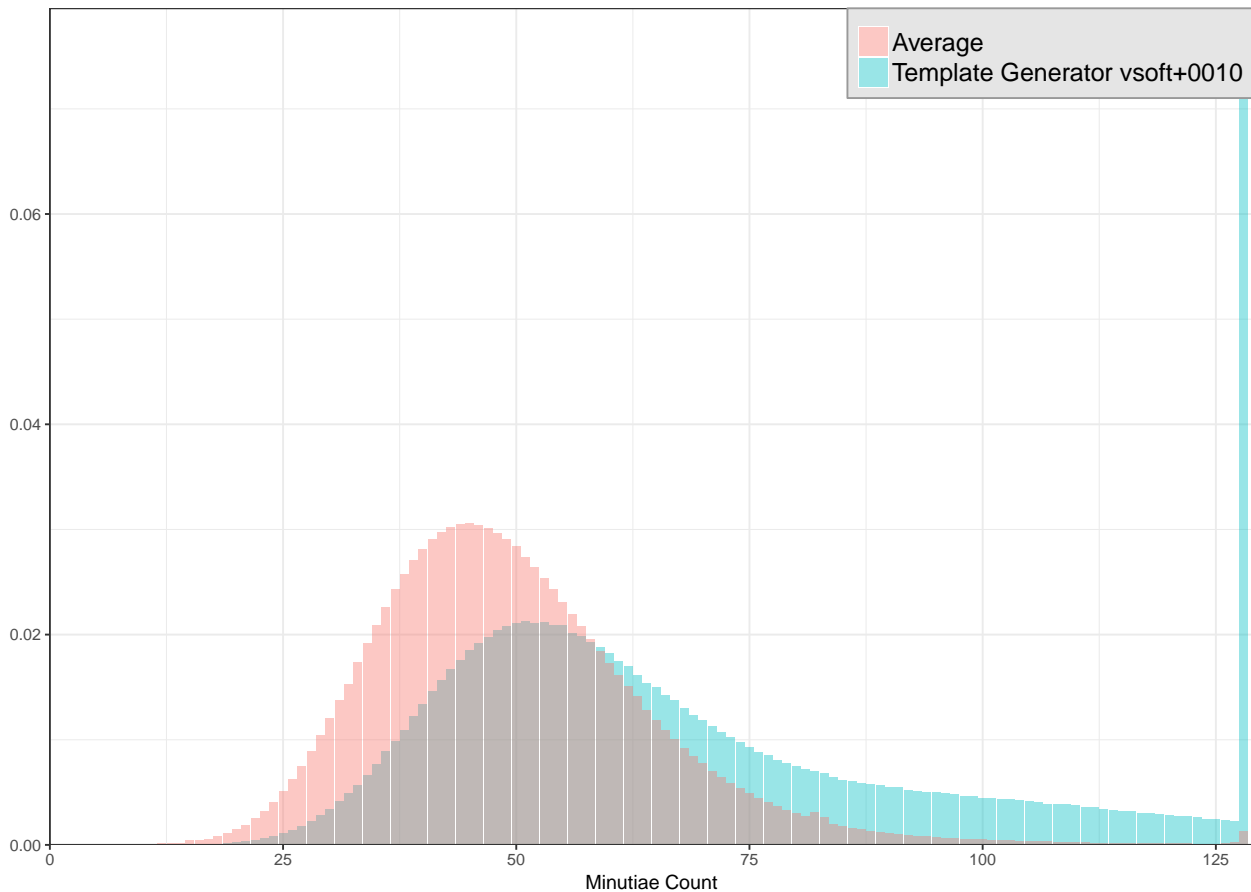


Figure 3: Probability distribution of the number of minutia the template generator found in the samples. The average probability distribution shows the combined distribution of minutia counts across all compliant template generators submitted for MINEX III (i.e., excluding Ongoing MINEX template generators).

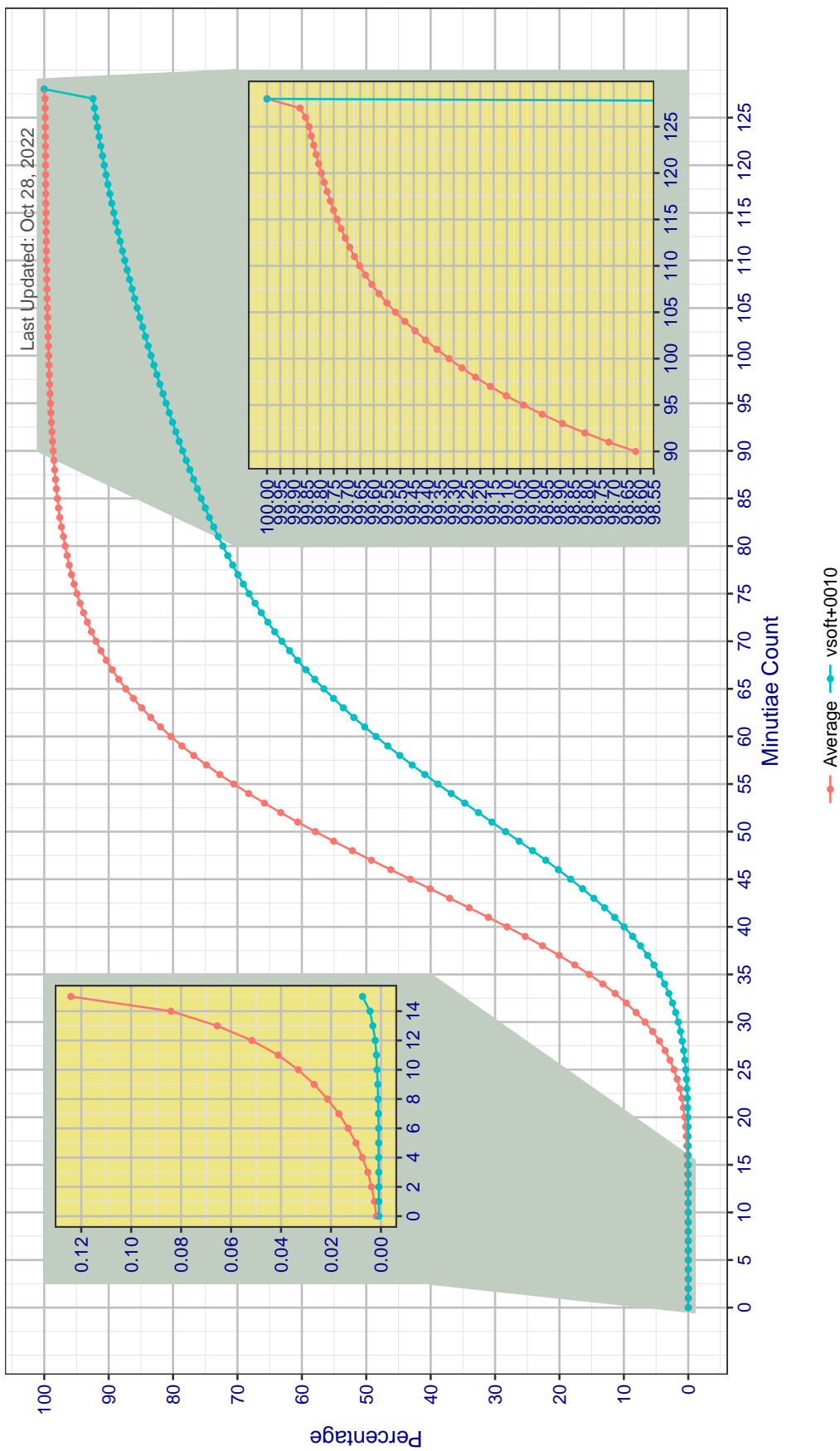


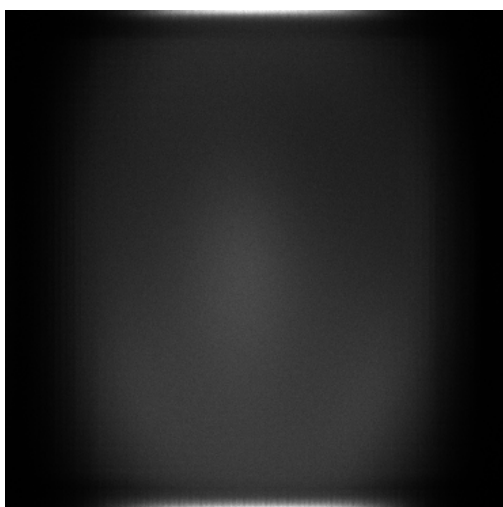
Figure 4: Cumulative summation of the number of minutiae the template generator found in the samples. The average probability distribution shows the combined distribution of minutiae counts across all compliant template generators submitted for MINEX III (i.e., excluding Ongoing MINEX template generators).

3.3 Minutia Density Plots

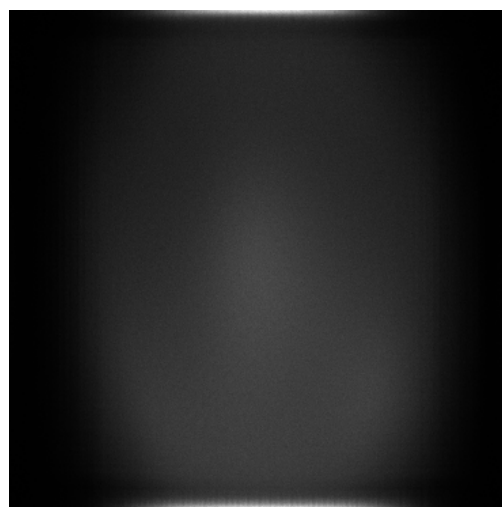
Minutia density plots show where the template generator tends to find minutia in fingerprint images. They are 2D histograms where the degree of illumination at an (x, y) coordinate indicates how frequently the software located a minutiae point at that location. The purpose of showing minutia density plots is to determine whether the template generator exhibits regional preference when locating minutia.

Some template generators produce minutia that exhibit a periodic structure, but this template generator does **not**. Periodic structures and other regional preferences are an indication that the template generator is departing from the minutia placement requirements of INCITS 378, clause 5. The expected pattern is a locally uniform distribution, and the appearance of local structure indicates systematic non-conformance with the standard. Given such behavior negatively affects interoperability[9], developers are asked to determine the cause of such behavior – for example, as an artifact of a tilebased image processing algorithms applied to the input fingerprint image – and to resubmit corrected algorithms.

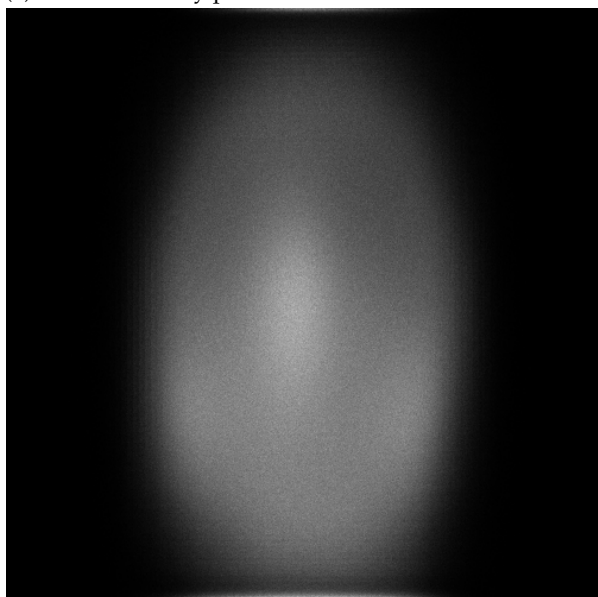
NIST uses a closed-form test to detect high frequency periodic structure by searching for modulation in the 368x368 minutia plot's Fourier representation. The code for this test is available [on GitHub](#).



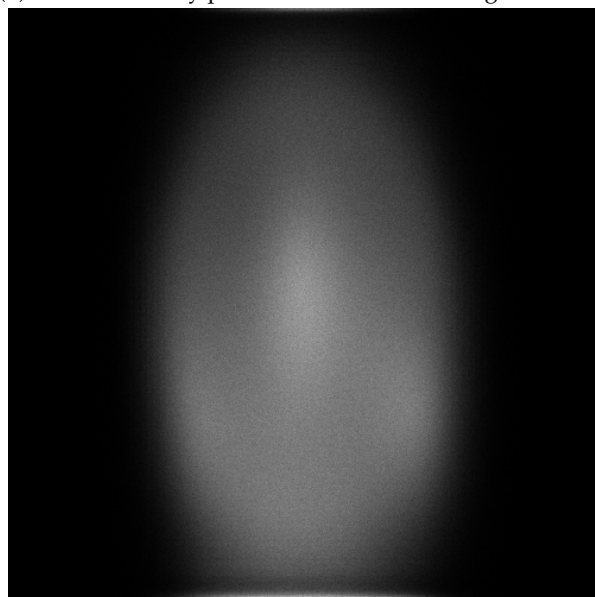
(a) Minutia density plot for 671 619 368x368 left indexes.



(b) Minutia density plot for 671 460 368x368 right indexes.



(c) Minutia density plot for 477 312 500x500 left indexes.



(d) Minutia density plot for 477 317 500x500 right indexes.

Figure 5: 2D Minutia Placement Density Functions.

4 References

- [1] Jonathan N. Bradley, Christopher M. Brislawn, and Thomas Hopper. FBI wavelet/scalar quantization standard for gray-scale fingerprint image compression. In *SPIE, Visual Information Processing II*, 1961. 3
- [2] George Doddington, Walter Liggett, Alvin Martin, Mark Przybocki, and Douglas Reynolds. Sheep, goats, lambs and wolves a statistical analysis of speaker performance in the nist 1998 speaker recognition evaluation. In *INTERNATIONAL CONFERENCE ON SPOKEN LANGUAGE PROCESSING*, 1998. 3
- [3] Patrick Grother Elham Tabassi, George W. Quinn. When to fuse two biometrics. In *IEEE Computer Society on Computer Vision and Pattern Recognition, Workshop on Multi-Biometrics*, 2006. 3
- [4] Robert Fontana, Giovanni Pistone, and Maria Rogantin. Classification of two-level factorial fractions. *Journal of Statistical Planning and Inference*, 87:149–172, 2000. 3
- [5] P. Grother, M. McCabe, C. Watson, M. Indovina, W. Salamon, P. Flanagan, E. Tabassi, E. Newton, and C. Wilson. Performance and Interoperability of the INCITS 378 Fingerprint Template. Technical report, NIST, 2006. 4
- [6] Olaf Henniger and Dirk Scheuermann. Minutiae template conformance and interoperability issues. In Arslan Brömme, Christoph Busch, and Detlef Hühnlein, editors, *BIOSIG*, volume 108 of *LNI*, pages 25–32. GI, 2007. 6
- [7] A. Martin, G. Doddington, T. Kamm, M. Ordowski, and M. Przybocki. The DET curve in assessment of detection task performance. In *Proc. Eurospeech*, pages 1895–1898, 1997. 3
- [8] George W. Quinn. Evaluation of latent fingerprint technologies: Fusion. In *NIST Latent Fingerprint Testing Workshop Recognition, Workshop*, 2009. 3
- [9] Elham Tabassi, Patrick Grother, Wayne Salamon, and Craig Watson. Minutiae interoperability. In Arslan Brömme, Christoph Busch, and Detlef Hühnlein, editors, *BIOSIG*, volume 155 of *LNI*, pages 13–30. GI, 2009. 6, 8
- [10] Edwin B. Wilson. Probable Inference, the Law of Succession, and Statistical Inference. *Journal of the American Statistical Association*, 22(158):209–212, 1927. 3